Suplemento de la Revista Mexicana de Física **3** 040918 (2022) 1–6

Synthesis of light nuclei in hadronic collisions

Harald Appelshäuser for the ALICE Collaboration

Institut für Kernphysik, Goethe-Universität Frankfurt, Max-von-Laue Strasse 1, 60438 Frankfurt am Main, Germany.

Received 3 July 2022; accepted 15 September 2022

Light-nuclei production yields in heavy-ion collisions are well described in the framework of Statistical Hadronization Models (SHM) but a thorough understanding of the underlying dynamics is still missing. In a complementary approach, synthesis of light nuclei can be modeled in terms of final-state coalescence of nucleons. While yielding an equally good description in central heavy-ion collisions, coalescence predictions are substantially different to those from SHM in small collision systems, in particular for the loosely bound hypertriton. This should allow a firm distinction of the two production scenarios in small collision systems. Comprehensive data on light-nuclei and hypertriton production in pp and p–Pb collisions from the ALICE Collaboration are presented in this contribution. Complementary to the measurement of production yields, the dynamics of nuclear cluster formation can be inferred from the measurement of final-state correlations of nucleons and light nuclei. Preliminary p-d correlation results from high-multiplicity pp collisions at $\sqrt{s} = 13$ TeV are compared to calculations based on experimental scattering parameters and discussed in the context of nuclear cluster formation.

Keywords: Light (anti)nuclei; (anti)hypernuclei; hypertriton; statistical hadronization model; coalescence; femtoscopy; hadron-hadron interactions.

1. Introduction

Measured hadron production yields in central Pb–Pb collisions at the LHC and predictions of Statistical Hadronization Models (SHM) [1] are in remarkable agreement over nine orders of magnitude[i] [2–7]. The grand-canonical description requires only two parameters, the hadron formation temperature (T) and the chemical potential of baryons (μ_B). Best agreement with the data is found for values of T that are compatible with the expected pseudo-critical temperature T_c from lattice QCD [8] while μ_B is very close to zero at LHC energies. This is astonishing since vacuum hadron masses are assumed in the model but masses are expected to change at temperatures around T_c. Moreover, all light nuclei and hypernuclei measured so far are also described within the SHM framework. While hadronic binding energies are at an energy scale compatible with T_c, (hyper)nuclear binding energies are about two orders of magnitude smaller. No dynamical picture exists that can reconcile the existence of loosely bound objects such as light nuclei in equilibrium at T_c.

In a complementary approach, the production of light nuclei can be described within so-called coalescence models [9, 10] (CM) in terms of nuclear cluster formation after the freeze-out of hadrons. In such models, light nuclei are formed when nucleons are sufficiently close in momentum space. State-of-the-art CMs consider (relative) length scales of the particle source and the size of the nuclear cluster [11, 12]. If the source size is smaller than the cluster size, the production yields are expected to be significantly suppressed in CMs. This makes a strong case for experimental exploration of light nuclei production in small collision systems like pp or p–Pb to test the coalescence picture. However, production rates of nuclei in small collision systems are small. Only recent experimental progress allowed the measurement of light nuclei and, most notably, hypertriton production in pp and p–Pb collisions by ALICE.

Alternatively, the dynamics of nuclear cluster formation can also be inferred from final-state momentum correlations of nucleons and light nuclei. A powerful framework for correlation analyses of final-state hadrons was developed in ALICE, yielding unique information on the characteristics of the hadron-emitting source and the mutual interaction among them. This so-called femtoscopy technique was recently extended to the light-nucleon sector. Preliminary results on final-state momentum correlations between protons and deuterons, emerging from high-multiplicity pp collisions at $\sqrt{s} = 13$ TeV, are presented in this contribution.

2. Particle ratios

Coalescence models can be tested by comparing the yields of light nuclei to that of protons. Recent data from ALICE on deuteron, ^{3}H and ^{3}He production indicate that cluster formation relative to protons is indeed suppressed in pp and p–Pb collisions at the LHC [13]. The observed system size dependence is compatible with CM calculations. On the other hand, canonical SHM [14] can describe the data as well, albeit at the expense of an additional parameter, *i.e.* in terms of a correlation volume V_c that describes the volume over which the conservation of charges is assumed.

Further insight can be gained by considering ratios of isobars in small collision systems. As an example, $^3\mathrm{H}/^3\mathrm{He} \approx 1$ is expected in SHM due to the almost identical masses of the two nuclei. In contrast, CM predicts $^3\mathrm{H}/^3\mathrm{He} > 1$ because of

---

i The heaviest particle included in the SHM analysis so far is the (anti-) $^4\mathrm{He}$ nucleus which is produced once in about 10^6 central Pb–Pb collisions. This corresponds to a production cross section similar to that of the Higgs boson.

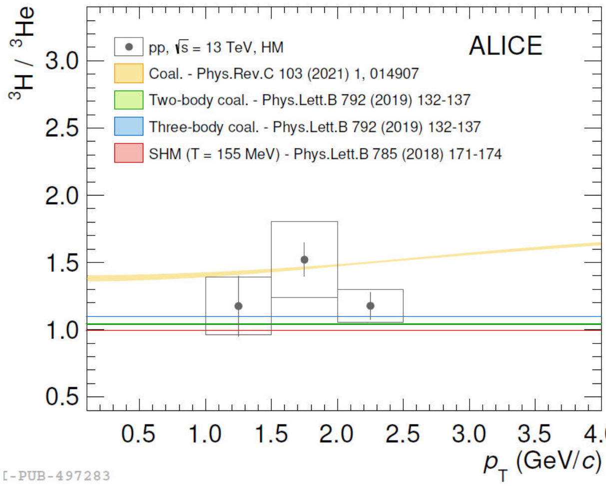

FIGURE 1. The $^{3}\mathrm{H}/^{3}\mathrm{He}$ ratio as a function of transverse momentum (p_{T}) in high-multiplicity pp collisions at $\sqrt{s}$ = 13 TeV [15]. The lines show calculations by SHM [14] and different coalescence models [11, 12].

the different matter radii of the two isobars: $r_{^3\mathrm{H}}/r_{^3\mathrm{He}} \approx 0.9$. First data on $^{3}\mathrm{H}/^{3}\mathrm{He}$ in high-multiplicity (HM) pp collisions at $\sqrt{s}$ = 13 TeV are available from ALICE [15], see Fig. 1. Within uncertainties, the ratio $^{3}\mathrm{H}/^{3}\mathrm{He}$ is still compatible with both SHM and CM calculations. Improved measurements with smaller uncertainties are expected from the upgraded ALICE detector in the near future.

The hypertriton is of particular interest in this context. It is the lightest known hypernucleus, composed of a proton, a neutron and a Λ hyperon. The properties of the hypertriton are governed by two-and three-particle forces between nucleons and the Λ. Preliminary results for the hypertriton lifetime measured in Pb–Pb collisions by ALICE [16] surpass the

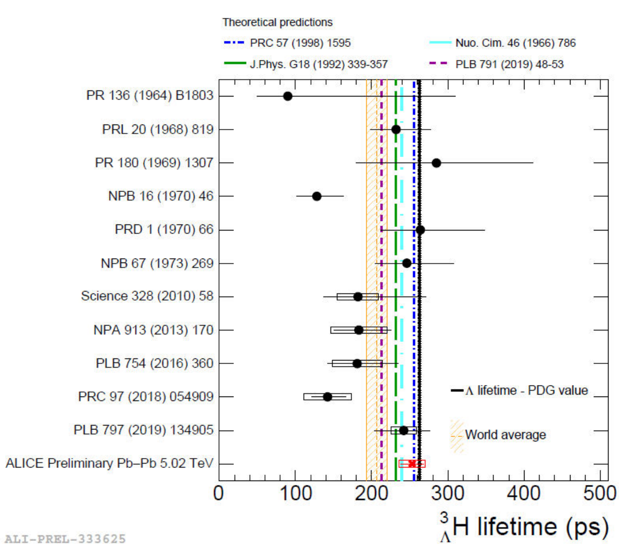

FIGURE 2. Collection of the hypertriton lifetime measurements obtained from different experiments [16]. The orange band represents the average of the lifetime values and the corresponding 1σ uncertainty. The dashed-dotted lines show different theoretical predictions.

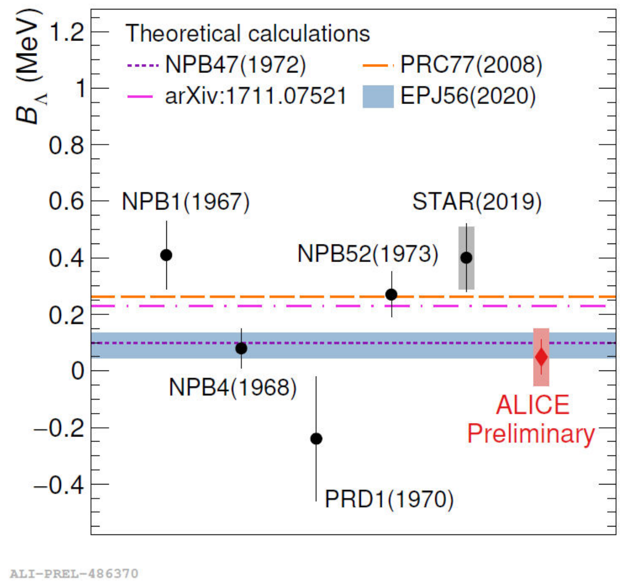

FIGURE 3. Binding energy of the Λ to the deuteron core of the hypertriton compared to theoretical predictions [17].

precision of all previous measurements and are compatible with the free-Λ lifetime (see Fig. 2). This resolves the long-standing "hypertriton lifetime puzzle". High-precision mass spectroscopy of the hypertriton allows also to extract the binding energy of the Λ to the deuteron core and confirms that the hypertriton is a very weakly bound object [17], see Fig. 3. Based on the small Λ separation energy it is expected that the Λ forms a halo around the deuteron core, leading to an RMS radius of the hypertriton that is by a factor 3-5 larger than that of ^{3}H or ^{3}He.

This property makes it an ideal probe to study cluster formation in small collision systems. The production of the hypertriton relative to that of ^{3}He can be studied in terms of the ratio $S_3 = (^{3}_{\Lambda}\mathrm{H}/^{3}\mathrm{He})/(\Lambda/p)$ where the penalty factor due to the mass difference drops out and possible size effects can be explored. While SHM and CM predict similar values for S_3 in central Pb–Pb collisions, large differences by about one order of magnitude or more are expected in pp and p–Pb.

First observation of the hypertriton in p–Pb and pp collisions was recently reported by ALICE [18, 19]. Hypertritons are reconstructed in the weak decay channel $^{3}_{\Lambda}\mathrm{H} \rightarrow {}^{3}\mathrm{He} + \pi^{-}$, where a branching ratio of 0.25 ± 0.02 is assumed. Advanced machine learning techniques allow the extraction of a significant hypertriton signal in p–Pb collisions at $\sqrt{s_{\mathrm{NN}}}$ = 5.02 TeV. In pp collisions, hypertritons are reconstructed in a dedicated high-multiplicity event sample at $\sqrt{s}$ = 13 TeV, see Fig. 4.

Combined with the measurement of ^{3}He, Λ and p, S_3 can be determined for the first time in small collision systems, see Fig. 5.

While the result in central Pb–Pb collisions [20] is compatible with both SHM [14] and CM [11] calculations, the new results in p-Pb and the preliminary result in pp favor the

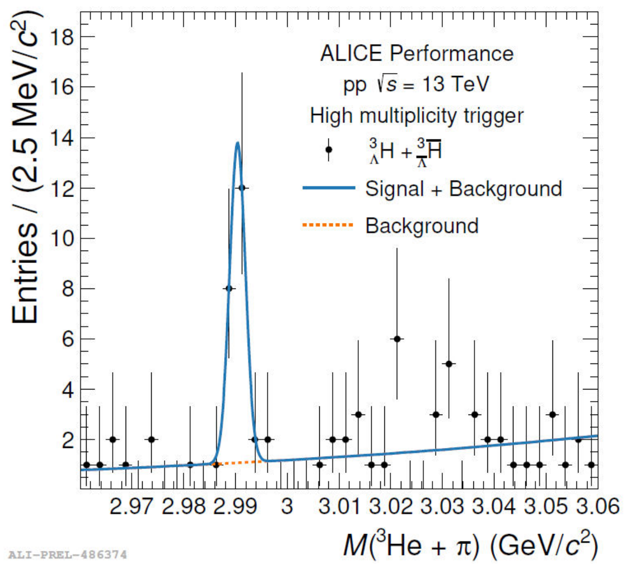

FIGURE 4. Invariant-mass distribution of $^{3}\mathrm{He}+\pi$ in HM pp collisions at $\sqrt{s}=13$ TeV [19].

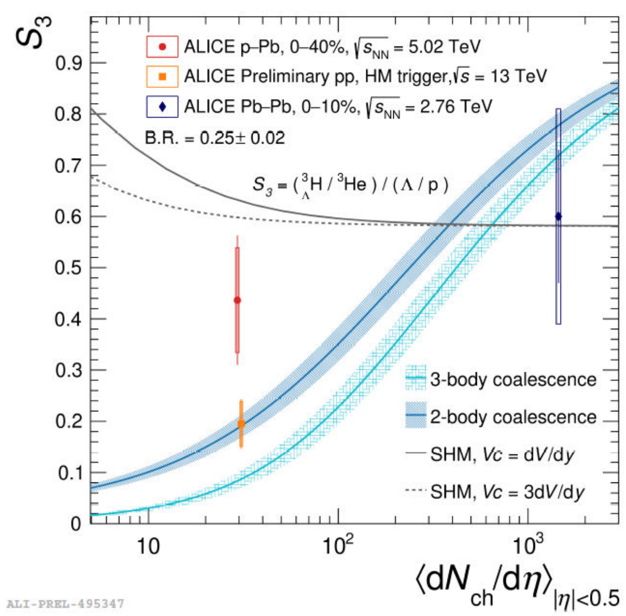

FIGURE 5. The ratio S_3 in HM pp collisions at $\sqrt{s}=13$ TeV, p–Pb collisions (0-40%) at $\sqrt{s_{\mathrm{NN}}}=5.02$ TeV and Pb–Pb collisions (0-10%) at $\sqrt{s_{\mathrm{NN}}}=2.76$ TeV collisions compared to calculations from SHM [14] and CM [11].

coalescence scenario. Future studies with higher precision may allow to further distinguish between two-body coalescence, where a more compact pre-formed deuteron combines with a Λ, and three-body coalescence, where all three baryons are projected on the large wave function of the hypertriton.

3. Femtoscopy

A complementary approach to study the dynamics of nuclear cluster formation employs the femtoscopy technique [21] where final-state momentum correlations of produced hadrons are investigated. The two-particle correlation function $C(k^*)$ is determined experimentally by the normalized ratio of correlated particle pairs from the same event and uncorrelated particle pairs from different ("mixed") events,

$$C(k^*) = A\frac{N_{\mathrm{same}}(k^*)}{N_{\mathrm{mixed}}(k^*)}, \tag{1}$$

where k^* is the momentum difference of the two particles in their rest frame. The full two-particle wave function $\Psi(k^*, r^*)$ including quantum correlations and interactions, integrated over the particle source distribution $S(r^*)$, is encoded in the correlation function:

$$C(k^*) = \int S(r^*)|\Psi(k^*, r^*)|^2 \mathrm{d}^3 r^*. \tag{2}$$

If the strong and electromagnetic final-state interactions between the particles are sufficiently well known, the measurement of $C(k^*)$ allows the determination of the characteristics of the particle source $S(r^*)$. Such Hanbury Brown-Twiss interferometry analyses using e.g. pairs of identical pions or protons were used extensively in the past decades to determine source sizes and lengths of homogeneity in various collison systems and over a wide range of energies.

A recent example of proton-proton correlations measured in HM pp collisions at $\sqrt{s}=13$ TeV by ALICE is shown in Fig. 6 [22]. Excellent description of the correlation function is achieved if Coulomb and strong final state interactions, employing the Argonne v_{18} potential [23] and Fermi-Dirac quantum statistics, is assumed. The only free parameter is the RMS radius of the Gaussian particle source which can be extracted from a fit of (2) to the data.

On the other hand, if the source function $S(r^*)$ is sufficiently well characterized and the assumption of a common source for different particle species is justified, femtoscopy can be used to study the final-state correlations of particle

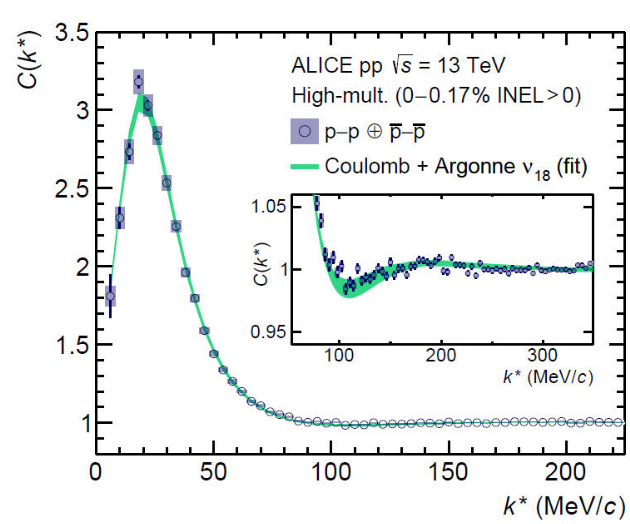

FIGURE 6. Measured p-p correlation function in HM pp collisions at $\sqrt{s}=13$ TeV measured by ALICE [22].

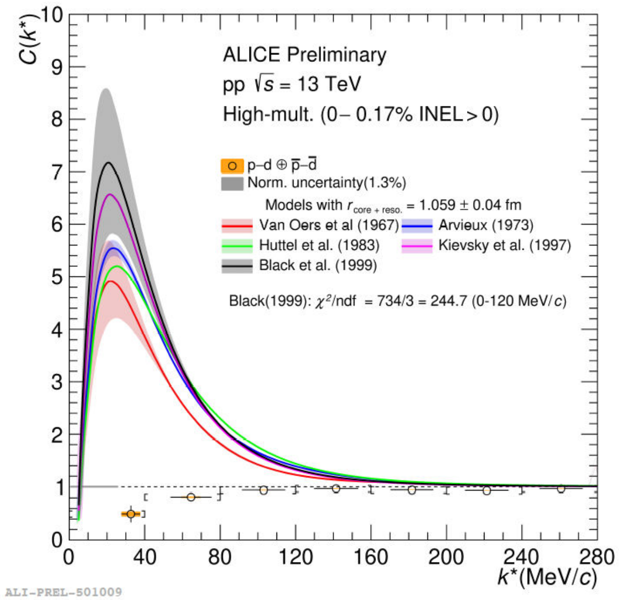

FIGURE 7. Preliminary p-d correlation function measured in HM pp collisions at $\sqrt{s} = 13$ TeV. Also shown are calculated correlation functions following the Lednicky-Lyuboshits approach using p-d scattering parameters from different experiments.

types where the interaction is yet unknown. This is of particular interest for short-lived particle species where precision scattering experiments can not be performed. A series of such femtoscopic analyses has been performed by ALICE in the recent years, among them precision measurements of the p-Λ, p-Ξ and p-Ω interactions [24, 25] which are of prime interest for the equation of state of neutron stars. Femtoscopic measurements can also shed light on coupled-channel dynamics in N-K [26, 27] and N-Λ [28] interactions. Moreover, first constraints on the p-ϕ [29] and p-D [30] interactions could be obtained from femtoscopy. These measurements are not discussed in detail here but they constitute a major step forward in the field of hadron physics and the understanding of hadronic interactions. They also manifest that femtoscopy is a powerful and consistent framework for the study of the particle source created in hadron and nuclear collisions and the final-state dynamics of the emitted hadrons.

New territory is entered if light nuclei are included in the femtoscopic measurements. In particular if scattering data exist, as is the case in the p-d system, comparison of the measured correlation function to calculations can give access to details of the light-nuclei formation process and to three-body interactions.

In Fig. 7 the p-d correlation function, measured in high-multiplicity pp collisions at $\sqrt{s} = 13$ TeV by ALICE is shown. The preliminary data exhibit a depletion below $k^* = 40$ MeV/c and are compatible with unity for larger k^*. Also shown in Fig. C7 are results from a calculation employing the Lednicky-Lyuboshits [31] prescription and using scattering parameters from different experiments. A source radius of 1.059 ± 0.04 fm is used in all calculations. This number was extracted from p-p correlations in high-multiplicity pp collisons at $\sqrt{s} = 13$ TeV measured at the same $\langle m_T \rangle$ as in the present p-d correlation analysis, following the conjecture of a common baryon source in pp collisions [32].

The model calculations clearly miss the data by far. Possible explanations could be related to a delayed formation of the deuteron, *e.g.* by coalescence, leading to a larger effective source size and reduced final-state interactions. On the other hand, the Lednicky-Lyuboshits approach may be inadequate for the treatment of composite objects like nuclear clusters if the size of the cluster exceeds that of the emission source. This demands for a more elaborate theoretical treatment, including full consideration of two- and three-body interactions and quantum effects, before final conclusions from the present findings can be drawn.

4. Summary

The production yields of light nuclei in the final state of central Pb–Pb collisions at the LHC are well reproduced by Statistical Hadronization Models, but the dynamics of nuclear cluster formation remains unclear. Coalescence models yield an equally good description in central Pb-Pb collisions, but the underlying picture is different since cluster formation is considered a post-freeze-out process. On the other hand, coalescence models include characteristic length scales which can be probed experimentally by varying the system size. The hypertriton is an exceptional tool for such studies because it is a loosely bound object with very large spatial extension. Pioneering measurements of hypertriton production in p–Pb and pp by ALICE are presented here. The results are in agreement with coalescence models while they tend to disfavor SHM, at least in small collision systems.

In a complementary approach, the final-state dynamics of cluster formation can be probed by femtoscopic measurements. Preliminary results on p-d correlations in high-multiplicity pp collisions can not be described within the Lednicky-Lyuboshits framework assuming measured scattering parameters and a common source of baryons. This may point to more complicated dynamics and the need for further theoretical developments.

The ALICE detector recently completed a major upgrade of its main subsystems which will allow to increase statistics by about two orders of magnitude in the coming years. Precision measurements of light nuclei and hypernuclei production as well as of femtoscopic correlations, including also hyperons and $A = 3$ nuclei, will significantly deepen the understanding of the synthesis of nuclei in hadronic and nuclear collisions.

1. A.Andronic, P. Braun-Munzinger, J. Stachel, H. Stöcker, Production of light nuclei, hypernuclei and their antiparticles in relativistic nuclear collisions, Phys. Lett. B697 (2011) 203, https://doi.org/10.1016/j.physletb.2011.01.053
2. S. Wheaton and J. Cleymans, THERMUS: A Thermal model package for ROOT, Comput. Phys. Commun. 180 (2009) 84, https://doi.org/10.1016/j.cpc.2008.08.001
3. A. Andronic, P. Braun-Munzinger, and J. Stachel, Thermal hadron production in relativistic nuclear collisions: The Hadron mass spectrum, the horn, and the QCD phase transition, Phys. Lett. B673 (2009) 142, https://doi.org/10.1016/j.physletb.2009.02.014, https://doi.org/10.1016/j.physletb.2009.06.021
4. A. Andronic, et al., Decoding the phase structure of QCD via particle production at high energy, Nature 561 (2018) 321, https://doi.org/10.1038/s41586-018-0491-6
5. G. Torrieri, et al., SHARE: Statistical hadronization with resonances, Comput. Phys. Commun. 167 (2005) 229, https://doi.org/10.1016/j.cpc.2005.01.004
6. G. Torrieri, et al., SHAREv2: Fluctuations and a comprehensive treatment of decay feed-down, Comput. Phys. Commun. 175 (2006) 635, https://doi.org/10.1016/j.cpc.2006.07.010
7. M. Petran, et al., SHARE with CHARM, Comput. Phys. Commun. 185 (2014) 2056, https://doi.org/10.1016/j.cpc.2014.02.026
8. A. Bazavov, et al., HotQCD Collaboration, Chiral crossover in QCD at zero and non-zero chemical potentials, Phys. Lett. B 795 (2019) 15, https://doi.org/10.1016/j.physletb.2019.05.013
9. R. Scheibl and U. Heinz, Coalescence and flow in ultrarelativistic heavy ion collisions, Physical Review C 59 (1999) 1585, https://doi.org/10.1103/physrevc.59.1585
10. J. I. Kapusta, Mechanisms for deuteron production in relativistic nuclear collisions, Phys. Rev. C21 (1980) 1301, https://doi.org/10.1103/PhysRevC.21.1301
11. K.-J. Sun, C. M. Ko, B. Dönigus, Suppression of light nuclei production in collisions of small systems at the Large Hadron Collider, Phys. Lett. B792 (2019) 132, https://doi.org/10.1016/j.physletb.2019.03.033
12. F. Bellini and A. P. Kalweit, Testing production scenarios for (anti-)(hyper-)nuclei and exotica at energies available at the CERN Large Hadron Collider, Phys. Rev. C 99 (2019) 054905, https://doi.org/10.1103/PhysRevC.99.054905
13. E. Bartsch, these proceedings.
14. V. Vovchenko, B. Dönigus, H. Stöcker, Multiplicity dependence of light nuclei production at LHC energies in the canonical statistical model, Phys. Lett. B785 (2018) 171, https://doi.org/10.1016/j.physletb.2018.08.041
15. ALICE Collaboration, S. Acharya et al., Production of light (anti)nuclei in pp collisions at $\sqrt{s} = 13$ TeV, JHEP 01 (2022) 106, https://doi.org/10.1007/JHEP01(2022)106
16. ALICE Collaboration, E. Bartsch et al., New results of light (anti-)(hyper-)nuclei production and hypertriton lifetime in Pb–Pb collisions at the LHC, Nucl. Phys. A 1005 (2021) 121791, https://doi.org/10.1016/j.nuclphysa.2020.121791
17. ALICE Collaboration, F. Mazzaschi et al., Quark Matter Conference 2022.
18. ALICE Collaboration, S. Acharya et al., Phys. Rev. Lett. 128 (2022) 25, 252003, https://doi.org/10.1103/PhysRevLett.128.252003
19. ALICE Collaboration, P. Fecchio et al., Strange Quark Matter Conference 2021.
20. ALICE Collaboration, S. Acharya et al., ${}^{3}_{\Lambda}\mathrm{H}$ and ${}^{3}_{\bar{\Lambda}}\bar{\mathrm{H}}$ production in Pb-Pb collisions at $\sqrt{s_{\mathrm{NN}}} = 2.76$ TeV, Phys. Lett. B 754 (2016) 360-372, https://doi.org/10.48550/arXiv.1506.08453
21. M. Lisa, S. Pratt, R. Soltz, U. Wiedemann, Femtoscopy in relativistic heavy ion collisions, Ann. Rev. Nucl. Part. Sci. 55 (2005) 357-402, https://doi.org/10.1146/annurev.nucl.55.090704.151533
22. ALICE Collaboration, S. Acharya et al., Investigation of the p-Σ^0 interaction via femtoscopy in pp collisions, Phys. Lett. B 805 (2020) 135419, https://doi.org/10.1016/j.physletb.2020.135419
23. R.B. Wiringa, V.G.J. Stoks, R. Schiavilla, An Accurate nucleon-nucleon potential with charge independence breaking, Phys. Rev. C 51 (1995) 38-51, https://doi.org/10.1103/PhysRevC.51.38
24. ALICE Collaboration, S. Acharya et al., p-p, p-Λ and Λ-Λ correlations studied via femtoscopy in pp reactions at $\sqrt{s} = 7$ TeV, Phys. Rev. C 99 (2019) 2, 024001, https://doi.org/10.1103/PhysRevC.99.024001
25. ALICE Collaboration, S. Acharya, et al., Unveiling the strong interaction among hadrons at the LHC, Nature 588 (2020) 232-238, Nature 590 (2021) E13 (erratum), https://doi.org/10.1038/s41586-020-3001-6, https://doi.org/10.1038/s41586-020-03142-2
26. ALICE Collaboration, S. Acharya et al., Scattering studies with low-energy kaon-proton femtoscopy in proton-proton collisions at the LHC, Phys. Rev. Lett. 124 (2020) 9, 092301, https://doi.org/10.1103/PhysRevLett.124.092301
27. ALICE Collaboration, S. Acharya et al., Kaon-proton strong interaction at low relative momentum via femtoscopy in Pb-Pb collisions at the LHC, Phys. Lett. B 822 (2021) 136708, https://doi.org/10.1016/j.physletb.2021.136708
28. ALICE Collaboration, S. Acharya et al., Exploring the NΛ-NΣ coupled system with high precision correlation techniques at the LHC, Phys. Lett. B 833 (2022) 137272, https://doi.org/10.1016/j.physletb.2022.13727
29. ALICE Collaboration, S. Acharya et al., Experimental Evidence for an Attractive p-ϕ Interaction, Phys. Rev. Lett. 127 (2021) 17, 172301, https://doi.org/10.1103/PhysRevLett.127.172301
30. ALICE Collaboration, S. Acharya et al., First study of the two-body scattering involving charm hadrons, https://arxiv.org/abs/2201.05352.

31. R. Lednicky and V.L. Lyuboshits, Final State Interaction Effect on Pairing Correlations Between Particles with Small Relative Momenta, Sov.J.Nucl.Phys. 35 (1982) 770, Yad.Fiz. 35 (1981) 1316-1330.

32. ALICE Collaboration, S. Acharya et al., Search for a common baryon source in high-multiplicity pp collisions at the LHC, Phys. Lett. B 811 (2020) 135849, https://doi.org/10.1016/j.physletb.2020.135849